Effect of bath temperature on the structural and optical properties of nickel sulphide (NiS) films prepared by chemical bath deposition

Jamal Basha K.A, Research Scholar, Department of Physics, Sri Venkateswara University, Tirupathi, India, jamalbashakhanahammad@gmail.com

Babu Pejjai, Professor, Department of Science and Humanities, Sri Venkateswara Engineering College, Karakambadi road, Tirupati, India, pdmj.babu@gmail.com

Ramakrishna Reddy K.T., Professor, Department of Physics, Sri Venkateswara University, Tirupathi, India, ktrkreddy@gmail.com

Abstract - Nickel sulphide (NiS) is a promising material, which can be used in different applications such as solar cells, super-capacitors, infra-red detectors and sensors. In the present study, NiS thin films were prepared at different bath temperatures (T_b), varying in the range of 50-80ºC by chemical bath deposition (CBD) method. The structural, morphological, elemental analysis, functional groups, and optical studies were carried out to examine the effect of bath temperature on the physical properties of NiS thin films. XRD studies revealed that the bath temperature had profound effect on the structure and crystallinity of CBD NiS films. The as-deposited NiS thin films showed amorphous nature at lower bath temperatures (<60ºC) whereas the diffraction pattern of NiS thin films deposited at $T_b \geq 70$ºC showed good crystallinity with hexagonal structure. The average crystalline size of the films was found to be 17 nm. The EDS analysis indicated the approach of stoichiometry with increase of T_b. The optical band gap energy of deposited NiS thin films was decreased from 2.25 eV to 2.03 eV with increase of bath temperature.

Keywords — Bath temperature, Band gap energy, Chemical bath, NiS thin films, Optical, Structural.

I. INTRODUCTION

The energy storage and conversion are the today's major needs of the entire world owing to the increased energy demand and partial accessibility of fossil fuels. In the present scenario, many researchers have focused to develop low cost and green energy storage, and conversion devices such as super capacitor and solar cells [1-3]. Mainly, the transition metal chalcogenides have been attracted much attention during the past decades due to their unique chemical and physical properties as well as their utilization as the catalytic, semiconducting, optical, and magnetic materials [4-8]. In the transition metal chalcogenides, metal sulfides such as the nickel sulphide (NiS), copper sulphide (CuS), zinc sulphide (ZnS), cadmium sulphide (CdS), silver sulphide (AgS) have been extensively studied and used in many applications [9-13]. Among these transition metal sulphides, NiS has been widely utilized in the application of energy storage and conversion devices. In nickel-sulfur system, different phases such as Ni_9S_8, Ni_7S_6, Ni_6S_5, Ni_3S_4, Ni_3S_2, NiS_2 and NiS have been reported. Among these phases, NiS exhibits two structures namely hexagonal α-NiS and rhombohedral β-NiS depending on the preparation conditions [14]. It has been used for many applications such as in solar cells [15], super-capacitors [16] and in lithium ion micro-batteries [17]. NiS is environmentally safe to handle and contains elements that are earth abundant.

NiS was prepared by various techniques such as a hydrothermal method [18], microwave synthesis [19], solvothermal method [20], precipitation method [21], spray pyrolysis method [22], ionic exchange process [23], screen printing method [24], polyol synthesis [25], reflux method [26] and chemical bath deposition method (CBD) [27]. Among these methods, chemical bath deposition has many advantages for the preparation of NiS thin films because it is simple, inexpensive method, suitable for the deposition of large surface area, wastage of material, usage of simple instruments and ease of control over doping of thin films. However, only few reports have been published so far on the deposition of NiS by CBD process with limited information on the film characteristics. Anuar Kassim et al. [28] studied the influence of triethanolamine usage on the properties of CBD grown NiS films. The study indicates

 DOI : 10.35291/2454-9150.2021.0524

that the number of peaks in the XRD data increased as the concentration of triethanolamine (TEA) was increased up to 0.1M. However, the XRD pattern of NiS films was not provided in that study. The SEM analysis indicates that the grains were much bigger for the films prepared using 0.1 and 0.2M of TEA than that of 0.05M. Paresh Gaikar et al.[27] prepared NiS films on Ti-substrate by chemical bath deposition method without any additive for pseudo capacitor application where the XRD pattern of NiS showed polycrystalline nature. In the CBD, among the various parameters, bath temperature is one of the most important factors that control the release of Ni and sulfur ions in the reaction bath during deposition. To the best of our knowledge, no reports have been published on the effect of bath temperature on the deposition and properties of NiS films deposited by CBD technique. Therefore in the present work, deposition of NiS thin films were carried out by using chemical bath deposition method at different bath temperature, which vary from 50ºC to 80ºC and the physical properties of the grown films were investigated.

II. EXPERIMENTAL

2.1. Preparation of NiS thin films

For the deposition of NiS films using CBD process, nickelsulphatehexahydrate ($NiSO_4{\cdot}6H_2O$) and thioacetamide (C_2H_5NS) were used as the precursors for nickel and sulphur ions. 20 ml of 0.8M $NiSO_4{\cdot}6H_2O$ aqueous solution was taken in a 100 ml beaker. To this solution, 4 ml of triethanolamine (TEA) was added drop wise. TEA acts as a complexing agent during the deposition period. The above mixture was stirred continuously for 15 min and then 4 ml of ammonia (NH_3) was added drop wise. Next, 20 ml of 0.8 M of thioacetamide aqueous solution was added to the above mixture. The pH of the solution was found to be about 9.5 after mixing the chemicals. Cleaning of the substrates prior to film deposition plays a crucial role in controlling the quality and adhesion of the deposited films. Therefore, the substrates were initially immersed in hot chromic acid for 30 min, cleaned using deionize water and then sonicated with doubled distilled water for another 15 min followed by drying in hot air oven. The pre-cleaned soda lime glass substrates were kept vertically in the chemical bath for the deposition of NiS films. The deposition was carried out at different bath temperatures varying in the range of 50-80 ºC for a fixed deposition time of 2 h. After deposition of films, the substrates were washed with distilled water, dried and used for characterization and analysis.

2.2. Characterization

The structure analysis of NiS films was carried out by using Rigaku X-ray diffractometer (Miniflex 600) using Cu k_α radiation in the 2θ range, 20º - 80º. The morphological and chemical compositions of the films were analyzed through the Scanning Electron Microscopy (JEOLJSM-IT500) along with the Energy Dispersive X-ray Spectroscopy (AMETEK). The functional groups present in the films were carried out using FTIR spectra (BRUKER) in the wave number range, 400 - 4000 cm^{-1}. The optical properties of NiS thin films were analyzed by using the UV-Vis spectrophotometer (SHIMADZU UV-2600i model) in the wavelength range of 450 – 850 nm.

III. RESULTS AND DISCUSSION

3.1. Structural studies

Fig.1shows the X-ray diffraction pattern of NiS thin films formed at various bath temperatures used in this study. The films grown at 50ºC showed amorphous nature with a broad hump observed near 25º. The films deposited at 60ºC showed two small peaks at 2θ = 30.74º and 54.15º that correspond to the (100) and (110) planes of hexagonal NiS. With increase of bath temperature an improvement in the crystallinity of NiS film can be observed. The diffraction pattern of NiS thin films deposited at 70ºC and 80ºC showed good crystallinity with hexagonal structure of space group P63/mnc. The diffraction pattern of NiS films deposited at bath temperatures ≥ 70ºC showed four peaks at 2θ = 30.10º, 34.47º, 45.79ºand 53.56º, which corresponds to the (100), (101), (102) and (110) planes, respectively. All the diffraction peaks were well matched with the hexagonal structure of NiS as reported in the JCPDS card number: 65-3419. No other impurity phases were observed in the XRD pattern, which suggests the high purity of CBD deposited NiS films. Out of the four crystal planes observed, the plane related to the (100) direction had the highest intensity, which indicated the preferred growth of this orientation. Further, the films deposited at 80ºC exhibited sharp and more intense (100) peak with low fringe width at half maximum compared to the films formed at 70 ºC, indicating good crystallinity in these films.

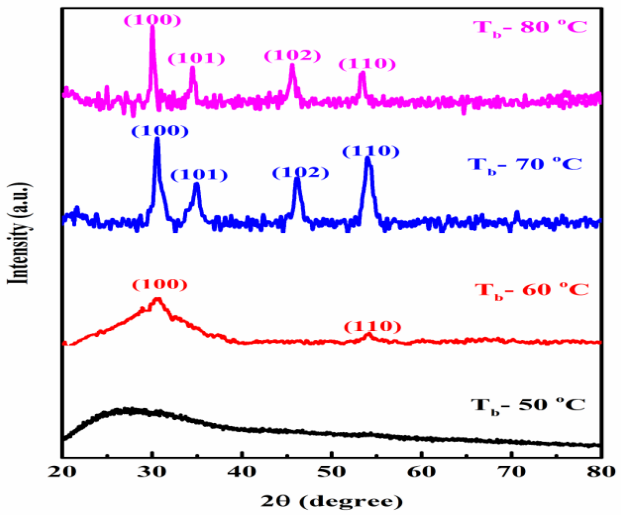

Fig. 1. X-ray diffraction pattern of NiS thin films at various bath temperatures.

 DOI : 10.35291/2454-9150.2021.0524

The average crystallite size was calculated using the Debye-Scherer equation,

$$D = \frac{0.9\,\lambda}{\beta \cos\theta}\ \text{nm}$$

Here, λ is the wavelength of X-rays used (Cu Kα radiation with λ = 1.542 Å), θ is the angle of diffraction and β is full width at half maxima. The average crystallite size of NiS films deposited at 70ºC and 80ºC was found to be 11 nm and 17 nm. As the bath temperature was increased, the kinetic energy of the reacting ions in the aqueous solution was increased that led to the nucleation of more ions in the crystallite with the result of an increase in the crystallite size.

The other structural parameters namely lattice parameters (a and c), micro-stain (ε), dislocation density (δ), positional parameters (u), bond length (l) and unit cell volume (V) of NiS thin films deposited at 70ºC and 80ºC were calculated using the relations given below [29-31]

$$\frac{1}{d^2} = \frac{4(h^2 + hk + k^2)}{3a^2} + \frac{l^2}{c^2}$$

$$\varepsilon = \frac{\beta}{4\tan\theta}$$

$$\delta = \frac{1}{D^2}\ \text{Lines/m}^2$$

$$u = a^2/3c^2 + 0.25$$

$$l = \sqrt{a^2/3 + \left(\frac{1}{2} - u\right)^2 c^2}$$

$$V = 0.866\ x a^2 x\ c$$

where, d_{hkl} is the inter-planar spacing; a and c are the lattice parameters; h, k, and l are the miller indices.

The evaluated crystallite size, micro strain, dislocation density, lattice constants (a & c), positional parameters, bond length and cell volume (a & c) of the prepared thin films were calculated from the XRD spectra and are listed in Table 1. The calculated lattice constants and other structural parameters of CBD NiS were found to be in close agreement with that of the reported NiS values [32].

Table 1: The structural parameters of NiS thin films prepared at various temperature.

Bath Temperature (ºC)	Diffraction peak	FWHM	Grain size (nm)	Dislocation density (10^{15}) Lines /m^2	Micro strain (10^{-3})	Lattice constant (a)	Lattice constant (c)	Positional parameter (u)	Bond length, l (Å)	Cell volume, V (Å)
70	(100)	0.0106	11	5.43	9.706	3.412	5.336	0.386	2.061	53.79
80	(100)	0.0068	17	2.25	6.300	3.423	5.373	0.385	2.085	54.20

3.2. Morphology analysis

The surface morphology of NiS thin films prepared at different bath temperatures is shown in Fig. 2 (a-d). The NiS thin films deposited at 50ºC showed particles with flake like structure. As can be seen from Fig. 2(a), the particles were agglomerated due to amorphous nature. The films deposited at 60ºC showed a layered structure and consist of beads shaped particles as shown in Fig. 2(b). The SEM image of NiS films formed at 70ºC exhibited completely different morphology compared to films deposited at 50ºC and 60ºC. The morphology of films, Fig. 2(c), grown at 70 ºC bath temperature revealed complete and dense coverage of the substrate with grains along with petals shaped particles over it. When the bath temperature was further increased to 80ºC, the surface of the deposited film showed agglomerated spherical and small rod shape particles as shown in Fig. 2(d). The change in the morphology with bath temperature was due to temperature effect on the nucleation growth of particles.

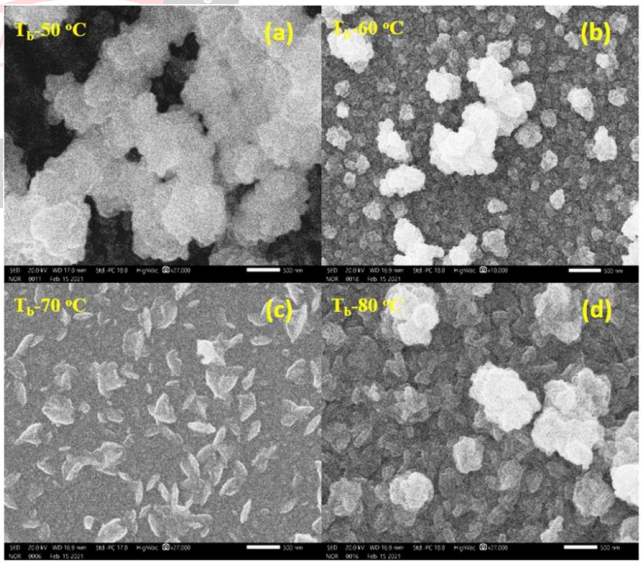

Fig. 2. Scanning electron microscope images of NiS films deposited at various bath temperatures.

3.3. Composition studies

The EDS spectra of NiS thin films deposited at different bath temperatures are shown in Fig.3 (a-d). It revealed that films deposited at 50ºC and 60ºC showed Ni and S along with O. The detection of oxygen in these layers might be

 DOI : 10.35291/2454-9150.2021.0524

due to the surface adsorption of oxygen or oxygen from $Ni(OH)_2$ formed along with NiS as such low temperatures may not be sufficient for complete reaction to occur in the solution. However, films prepared at bath temperatures in the range of 70-80°C showed only Ni and S, which indicates complete conversion of the bath mixture into NiS with increase of temperature. The composition of elements estimated for NiS films formed at different bath temperatures from the EDS spectra is given in Table 2.

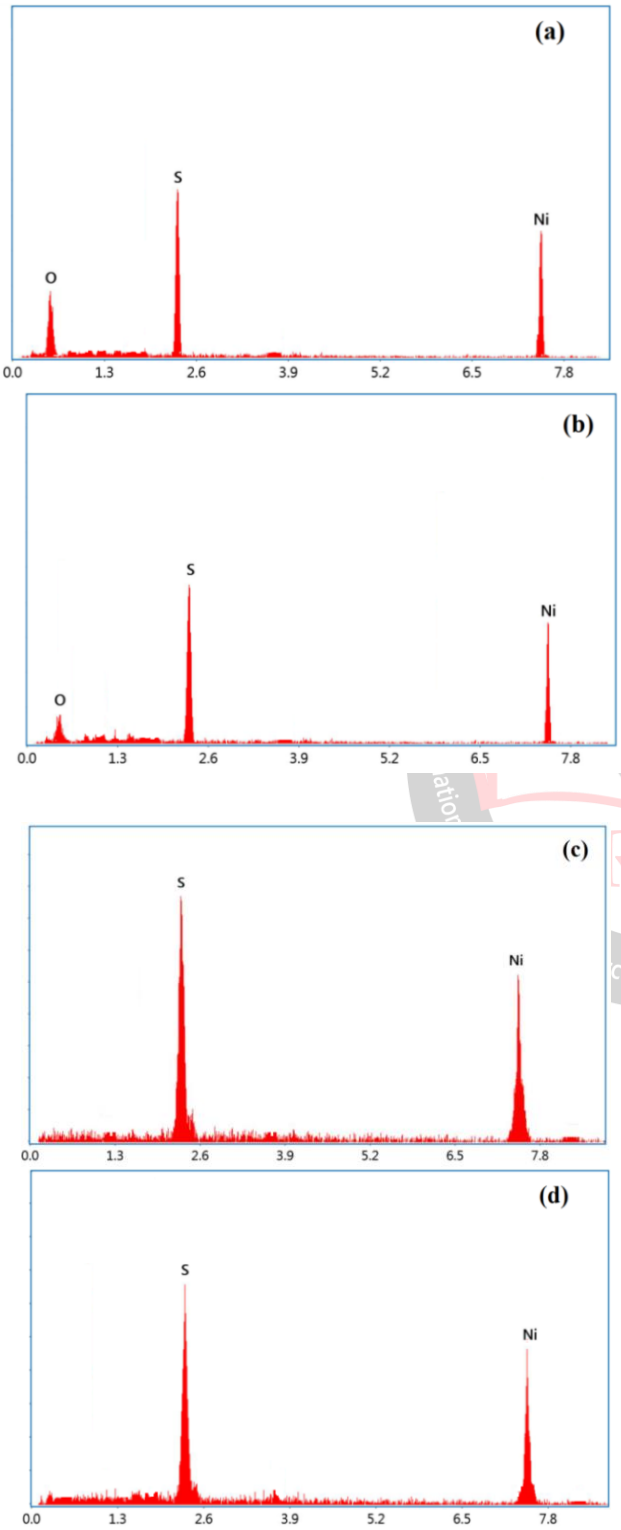

Fig. 3. EDS spectra of NiS films formed at T_b = (a) 50°C, (b) 60°C (c) 70°C and (d) 80°C.

Table 2: Measured elemental composition of NiS films using EDS.

Sl No	Bath temperature,	Atomic %			Ni/S
	T_b (°C)	O	S	Ni	
1	50	9.79	48.05	42.16	0.88
2	60	5.6	48.12	46.28	0.96
3	70	-	50.1	49.9	0.99
4	80	-	49.89	50.11	1.00

3.4. FTIR analysis

Fig. 4 represents the FTIR spectra of NiS films prepared at various bath temperatures. The spectra showed two major peaks at 456 cm^{-1} and 517 cm^{-1} related to Ni-S stretching vibrations. These peaks are in close agreement with the characteristics vibration modes of Ni-S, confirming the formation of NiS on the substrates [33, 25]. In general, the peaks observed close to 3600 cm^{-1} corresponds to the hydroxyl (OH) stretching vibration of the absorbed water molecules [34]. However, in the FTIR spectra of NiS layers deposited at 70°C and 80°C showed very small peaks in the wave number range of 3200-3600 cm^{-1}, which indicates the high quality of NiS films with very less water content in the layers.

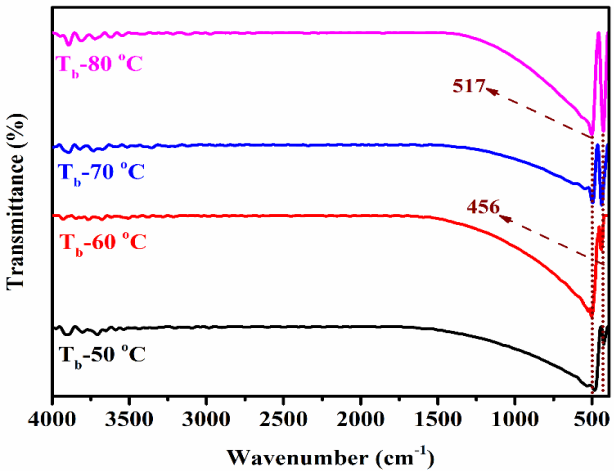

Fig. 4. FTIR spectra of NiS films deposited at various bath temperatures.

3.5. Optical properties

The absorbance spectra of NiS films deposited at different bath temperatures are shown in Fig.5. It can be observed from the figure that the optical absorbance is decreased sharply with increase of wavelength near the fundamental absorption region, indicating the direct nature of the energy band gap in these films. Also, there is an increase of absorption in the films with increase of bath temperature, which might be due to the increase of crystallite size in the films.

 DOI : 10.35291/2454-9150.2021.0524

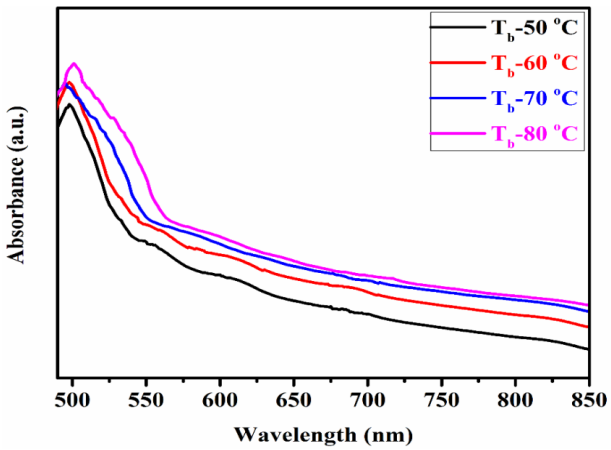

Fig. 5. Absorbance spectra of NiS thin films deposited at different bath temperatures.

The optical energy band gap of films was estimated through Tauc plots, which are shown in Fig. 6. The evaluated band gap energy of NiS layers deposited at 50ºC, 60ºC, 70ºC and 80ºC were found to be 2.25 eV, 2.15 eV, 2.06 eV and 2.03 eV respectively. The higher band gap values of 2.25 eV and 2.15eV determined for films deposited at 50ºC and 60ºC might be due to the presence of little amount of oxygen in the films in the form of NiO and $Ni(OH)_2$ phases as evident from EDS and FTIR analysis [35], although such phases were not noticed in the XRD. When the bath temperature was increased to 80ºC, the adsorbed water molecules were removed from the films, which led to a decrease of band gap to 2.03 eV [36]. These values of band gap energy of NiS films are in good agreement with that of bulk NiS [37] and reported values in thin films [38].

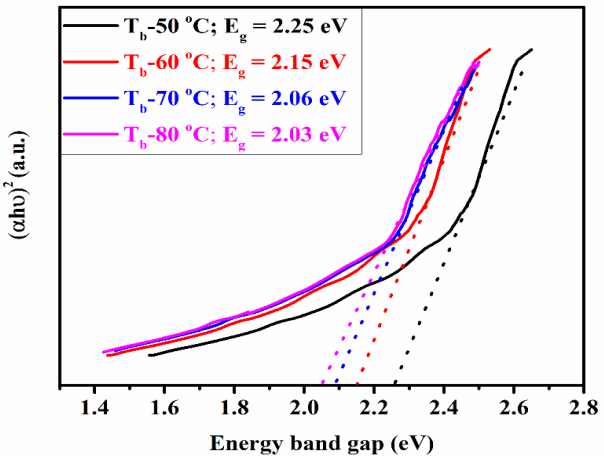

Fig. 6. Tauc's plots of NiSlayers formed at different bath temperatures.

Fig. 7 shows the spectral variation of refractive index, n and extinction coefficient, k of NiS films deposited at various bath temperatures as a function of wavelength. From Fig. 7(a), it is observed that the value of refractive index 'n' decreased with increase of wavelength and shifted towards the longer wavelengths as bath temperature increased to 80ºC. This might be due to decrease in packing density with increase of bath temperatures from 50ºC to 80ºC [39]. From Fig. 7(b), it is observed that the extinction coefficient falls sharply at the initial stage (λ ~ 520- 580 nm)) and thereafter its change is marginal above these wavelengths. The sharp decrease might be due to decrease in the optical scattering and absorbance. The initial decrease of 'k' values with wavelength indicates the light absorption at specific wavelengths as reported in the literature [40, 41].

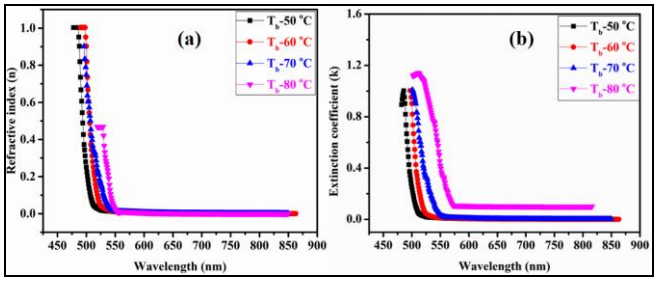

Fig. 7. Change of (a) refractive index and (b) extinction coefficient with wavelength in NiS films.

IV. CONCLUSIONS

The NiS thin films were successfully deposited by the chemical bath deposition method at different bath temperatures that vary in the range of 50ºC-80ºC. The XRD studies revealed amorphous nature in NiS layers for T_b < 70ºC and only single phase with an intense (100) plane along with hexagonal crystal structure for $T_b \geq 70$ºC. The SEM analysis showed bath temperature dependent growth of NiS particles with a change in the surface morphology. The EDS analysis indicated near stoichiometric composition for the layers deposited at T_b = 80ºC. The FTIR studies showed the characteristic vibrational modes of Ni-S. The optical band gap of the films was decreased from 2.25 eV to 2.03 eV with increase of bath temperature from 50ºC to 80ºC. The single phase, near stoichiometric and highly absorbing NiS films formed at T_b = 80ºC might be useful in the energy conversion and energy storage applications.

REFERENCES

[1] Godlaveeti SK, Maseed H, Reddy SA, Nagireddy RR. Electrochemical performance of ternary RGO/β-Ni(OH)2/CeO2composite in addition with different metal oxides for supercapacitor application, Adv. Nat. Sci. Nanosci. & Nanotechnol., 11 (2020) 025021. doi:10.1088/2043-6254/ab8bde.

[2] Godlaveeti SK, Jangiti S, Somala AR, Maseed H, Nagireddy RR. Different Phase and Morphology Effect of Manganese Oxide on Electrochemical Performance for Supercapacitor Application, J. Clust. Sci., 32 (2021) 703-710. doi:10.1007/s10876-020-01833-4.

[3] Patil SA, Hussain S, Shrestha NK, Mengal N, Jalalah M, Jung J, et al. Facile synthesis of cobalt–nickel sulfide thin film as a promising counter electrode for triiodide reduction in dye-sensitized solar cells, Energy, 202 (2020) 117730. doi:10.1016/j.energy.2020.117730.

[4] Majhi KC, Yadav M. Transition metal chalcogenides based nanocomposites as efficient electrocatalyst for hydrogen

 DOI : 10.35291/2454-9150.2021.0524

evolution reaction over the entire pH range, Int. J. Hydrogen Energy 45 (2020) 24219–31. doi:10.1016/j.ijhydene.2020.06.230.

[5] Yu X, Sivula K. Layered 2D semiconducting transition metal dichalcogenides for solar energy conversion, Curr. Opin. Electrochem. 2 (2017) 97–103. doi:10.1016/j.coelec.2017.03.007.

[6] Hwang Y, Choi J, Ha Y, Cho S, Park H. Electronic and optical properties of layered chalcogenide FeIn2Se4, Curr. Appl. Phys., 20 (2020) 212–218. doi:10.1016/j.cap.2019.11.005.

[7] Li H, Hu S, Zhao S, Lan C. First-principles study on the electronic and optical properties of 2D chalcogenides M2X and M2X3 (M = Tl, in and X = O, S, Se), Chem. Phys. Lett., 749 (2020) 137404. doi:10.1016/j.cplett.2020.137404.

[8] Feng LY, Villaos RAB, Cruzado HN, Huang ZQ, Hsu CH, Hsueh HC, et al. Magnetic and topological properties in hydrogenated transition metal dichalcogenide monolayers, Chinese J. Phys., 66 (2020) 15–23. doi:10.1016/j.cjph.2020.03.018.

[9] Ananth A, Han I, Akter M, Boo JH, Choi EH. Handy soft jet plasma as an effective technique for tailored preparation of ZnS nanomaterials and shape dependent antibacterial performance of ZnS, J. Ind. Eng. Chem., 90 (2020) 389–398. doi:10.1016/j.jiec.2020.07.042.

[10] Ahamad T, Naushad M, Alshheri SM. Fabrication of highly porous N/S doped carbon embedded with CuO/CuS nanoparticles for NH3 gas sensing, Mater. Lett., 268 (2020) 127515. doi:10.1016/j.matlet.2020.127515.

[11] Feng C, Chen Z, Jing J, Sun M, Tong H, Hou J. Band structure and enhanced photocatalytic degradation performance of Mg-doped CdS nanorods, Phys. B: Condens. Matter., 594 (2020) 412363. doi:10.1016/j.physb.2020.412363.

[12] Hamed MSG, Oseni SO, Kumar A, Sharma G, Mola GT. Nickel sulphide nano-composite assisted hole transport in thin film polymer solar cells, Solar Energy, 195 (2020) 310–317. doi:10.1016/j.solener.2019.11.068.

[13] Sadovnikov SI, Ishchenko A V., Weinstein IA. Synthesis and optical properties of nanostructured ZnS and heteronanostructures based on zinc and silver sulfides, J. Alloys and Compd., 831 (2020) 154846. doi:10.1016/j.jallcom.2020.154846.

[14] R.Ghaelbash, M.B.Sigman, B.A.Korgel, Solventless synthesis of nickel sulphide nanorods & traingular nanoprisms, Nano Lett., 4 (2004) 537-542.

[15] Li W, Chen Q, Zhong Q. One-pot fabrication of mesoporous g-C3N4/NiS co-catalyst counter electrodes for quantum-dot-sensitized solar cells, J. Mater. Sci., 55 (2020) 10712–10724. doi:10.1007/s10853-020-04672-w.

[16] Shombe GB, Khan MD, Zequine C, Zhao C, Gupta RK, Revaprasadu N. Direct solvent free synthesis of bare α-NiS, β-NiS and α-β-NiS composite as excellent electrocatalysts: Effect of self-capping on supercapacitance and overall water splitting activity, Sci. Rep., 10 (2020) 1–14. doi:10.1038/s41598-020-59714-9.

[17] Zhang Q, Peng G, Mwizerwa JP, Wan H, Cai L, Xu X, et al. Nickel sulfide anchored carbon nanotubes for all-solid-state lithium batteries with enhanced rate capability and cycling stability, J. Mater. Chem. A, 6 (2018) 12098–105. doi:10.1039/c8ta03449d.

[18] Xia G, Li X, Gu Y, Dong P, Zhang Y, Duan J, et al. Flower-like NiS/C as high-performance anode material for sodium-ion batteries, Ionics, 27 (2020) 191-197. doi.org/10.1007/s11581-020-03818-9.

[19] Nandhini S, A. JCM, Muralidharan G. Facile microwave-hydrothermal synthesis of NiS nanostructures for supercapacitor applications, Appl. Surf. Sci., 449 (2018) 485–491. doi:10.1016/j.apsusc.2018.01.024.

[20] Muninathan S, Arumugam S. Enhanced photocatalytic activities of NiS decorated reduced graphene oxide for hydrogen production and toxic dye degradation under visible light irradiation, Int. J. Hydrogen Energy, 46 (2021) 6532–6546. doi:10.1016/j.ijhydene.2020.11.178.

[21] Ryu HS, Ha CW, Ji SY, Ahn IS, Ahn JH, Ahn HJ, et al. Electrochemical properties of the NiS powder prepared by co-precipitation method for lithium secondary battery, J. Nanosci. Nanotechnol., 14 (2014) 7943–7947. doi:10.1166/jnn.2014.9458.

[22] Boughalmi R, Rahmani R, Boukhachem A, Amrani B, Driss-Khodja K, Amlouk M. Metallic behavior of NiS thin film under the structural, optical, electrical and ab initio investigation frameworks, Mater. Chem. Phys., 163 (2015) 99–106. doi:10.1016/j.matchemphys.2015.07.019.

[23] Yan X, Tong X, Ma L, Tian Y, Cai Y, Gong C, et al. Synthesis of porous NiS nanoflake arrays by ion exchange reaction from NiO and their high performance supercapacitor properties, Mater. Lett., 124 (2014) 133–136. doi:10.1016/j.matlet.2014.03.067.

[24] Kumar V, Sharma DK, Sharma K, Dwivedi DK. Investigation on physical properties of polycrystalline nickel sulphide films grown by simple & economical screen-printing method, Optik, 156 (2018) 43–48. doi:10.1016/j.ijleo.2017.10.169.

[25] Surendran S, Sankar KV, Berchmans LJ, Selvan RK. Polyol synthesis of α-NiS particles and its physico-chemical properties, Mater. Sci. Semicond. Process., 33 (2015) 16–23. doi:10.1016/j.mssp.2015.01.012.

[26] Qu C, Zhang L, Meng W, Liang Z, Zhu B, Dang D, et al. MOF-derived α-NiS nanorods on graphene as an electrode for high-energy-density supercapacitors, J. Mater. Chem. A, 6 (2018) 4003–4012. doi:10.1039/c7ta11100b.

[27] Gaikar P, Pawar SP, Mane RS, Nuashad Mu, Shinde DV. Synthesis of nickel sulfide as a promising electrode material for pseudocapacitor application, RSC Adv., 6 (2016) 112589-112593. doi.org/10.1039/C6RA22606J.

[28] Anuar Kassim, Ho Soon Min, Tan Wee Tee and Ngai Chee Fei, Influence of triethanolamine on the chemical bath

 DOI : 10.35291/2454-9150.2021.0524

deposited NiS thin films, American J. Appl. Sci., 8 (2011) 359-361.

[29] Sreenivasa Kumar G, Venkataramana B, Reddy SA, Maseed H, Nagireddy RR. Hydrothermal synthesis of Mn3O4nanoparticles by evaluation of pH effect on particle Size formation and its antibacterial activity, Adv. Nat. Sci. Nanosci. Nanotechnol., 11 (2020) 035006. doi:10.1088/2043-6254/ab9cac.

[30] Dhandayuthapani T, Sivakumar R, Sanjeeviraja C, Gopalakrishnan C, Arumugam S. Microstructure, optical and magnetic properties of micro-crystalline γ-MnS film prepared by chemical bath deposition method, Mater. Sci. Semicond. Process., 72 (2017) 67–71. doi:10.1016/j.mssp.2017.09.025.

[31] Mia MNH, Pervez MF, Hossain MK, Reefaz Rahman M, Uddin MJ, Al Mashud MA, et al. Influence of Mg content on tailoring optical bandgap of Mg-doped ZnO thin film prepared by sol-gel method, Results in Phys., 7 (2017) 2683–2691. doi:10.1016/j.rinp.2017.07.047.

[32] Jeng–Hang Wang, Zhe Cheng, jean-Luc Bredas, Meilin Liu, Electronic and vibrational propertiesof nickel sulphides from first principles, Chem. Phys., 127 (2007) 214705. https://doi.org/10.1063/1.2801985

[33] Bhardwaj R, Jha R. Trisodium citrate assisted morphology controlled synthesis of nickel sulphide nanoparticles with enhanced cyclic stability as carbonaceous free electrodematerial, Mater. Chem.Phys., 255 (2020) 123581. doi:10.1016/j.matchemphys.2020.123581.

[34] Zengjun Chen ,Tatjana Dedova ,Ilona Oja Acik ,Mati Danilson ,Malle Krunks, Nickel oxide films by chemical spray: Effect of deposition temperature and solvent type on structural, optical, and surface properties, Appl. Surf. Sci., 48 (2021) 149118. doi.org/10.1016/j.apsusc.2021.149118

[35] F.I. Ezema, A.B.C. Ekwealor, R.U. Osuji, Optical Properties of chemical bath deposited nickel oxide (NiO)X thin films, Superficies, 2008; 21: 6-10. *versión impresa* ISSN 1665-3521.

[36] M.M. Gomma, M.Boshta, B.S. Frag, M.B.S.Osman, Structural and optical properties of nickel oxide thin films prepared by chemical bath deposition and spray pyrolysis techniques, Mater. Sci.: Mater.Electron., 2015; 27; 711–717. doi 10.1007/s10854-015-3807-4

[37] M. Nakamura, A. Fujimori, M. Sacchi, J.C. Fuggle, A. Misu, T. Mamori, H. Tamura, M. Matoba, S. Anzai, Metal-nonmetal transition in NiS induced by Fe and Co substitution: X-ray-absorption spectroscopic study, Phys. Rev. B,48 (1993) 16942–16947. doi10.1103/physrevb.48.16942

[38] Sumanta Jana, Nillohit Mukherji, Biswajit Chakraborthy, Bibhas Chandra Mitra, Anup Mondal, Electrodeposited polymer encapsulated nickel sulphide thin films, Appl. Surf. Sci., 300 (2014) 300 154-156. doi.org/10.1016/j.apsusc.2014.02.026.

[39] E.R. Shaaban, M S Abd El-Sadek, M El-Hagary and I S Yahia, Spectroscopic ellipsometry investigations of the optical constants of nanocrystalline SnS thin films, Physica Scripta, 86 (2012) 015702. doi.org/10.1088/0031-8949/86/01/015702

[40] Sreedevi Gedi, Vasudeva Reddy Minnan Reddy, Chinho Park, Jeon Chan-Wook, Ramakrishna Reddy K.T., Comprehensive optical studies SnS layers synthesized by chemical bath deposition,Opt. Materials.,42 (2015) 468-475. doi.org/10.1016/j.optmat.2015.01.043.

[41] M.R.I. Chowdhury, J.Podder, and A.B.M.O. Isalm, Synthesis and characterization of manganese sulphide thin films deposited by spray pyrolysis, Cryst. Res. Technol., 46 (2011) 267-271. doi.org/10.1002/crat.201000549.

 DOI : 10.35291/2454-9150.2021.0524